논문 97-6-6-05

자기 이상검출 시스템의 신호 대 잡음비 개선을 위한 자기환경 필터 이론

김원호*, 김은로**, 양창섭**, 최인규***, 최준림***, 박종식***

A Theory of the Geological Magnetic Filter for the Improvement of the Signal to Noise Ratio of the Magnetic Detection System

Won-Ho Kim*, Eun-Ro Kim**, Chang-Sub Yang**, In-Kyu Choi***,
Jun-Rim Choi***, and Jong-Sik Park***

요 약

본 논문에서 자기 이상 검출시스템의 신호 대 잡음비 개선을 위하여 자기환경 필터의 이론을 제안하였다. 자기환경 필터는 검출센서와 기준센서로부터 자기장을 측정하여 주파수 공간에서 상관관계를 측정하여 구성된다. 이를 이용하면 간섭성 잡음을 제거시켜 신호대 잡음비를 개선시킬 수 있다. 최근의 DSP 하드웨어 기술을 이용하면 자기환경 필터의 하드웨어 구현이 용이하다.

컴퓨터 시뮬레이션을 통하여 여러 자기 환경 조건에서 제안된 자기환경 필터의 성능을 보였다. 시뮬레이션 결과 자기환경 필터는 간섭성 잡음을 소거시킬 뿐만 아니라 센서의 오배치에 의한 오차를 제거하고 지역적으로 국한된 규칙적인 잡음도 제거할 수 있음을 알 수 있었다.

Abstract

In this paper, a theory of the geological magnetic filter for the improvements of the signal to noise ratio of the magnetic detection system has been developed. The geological magnetic filter takes two sequences of magnetic fields measured from the reference sensor and the detector sensor and calculates the correlations between them in the frequency domain. Using the filter, we can remove the coherent noises in the time domain and improve the signal to noise ratio of the magnetic detection system. With the recent developments of the DSP hardware technology the geological magnetic filter can be easily implemented using the digital signal processor. We show the ability of the geological magnetic filter under various circumstances through computer simulations. Numerical simulation results show that geological magnetic filter can excellently remove the sensor misalignment effects and the regular short range local noise as well as it delete the coherent noises.

I. INTRODUCTION

Magnetic detection system detects the change of the short range magnetic fields generated by magnetic materials and identifies the existence of magnetic anomalies. The detecting ability of magnetic detection system is mainly determined

* 동의공업전문대학 전자과(Dept. of electronics, Dongeui Technical Junior College)
** 국방과학연구소(Agency for Defence Development)
*** 경북대학교 전자·전기공학부(Dept. of Electronics & Electrical Engineering, KyungPook Nat'l Univ.)
<접수일자 : 1997년 9월 1일>

by the sensitivity of the magnetic sensor. High sensitivity magnetic sensor has the sensitivity of about 10^{-10} gauss. Recently, the development of the high Tc superconductor enables the implementation of very sensitive magnetic detection system at the fair expense. With the increase of the sensitivity of the magnetic detection system, the DSP algorithms to increase the signal to noise ratio become more important. The sources of magnetic noises in the magnetic detection system are as follows;

- Time varying micropulsation fields of the earth magnetic fields.
- Low frequency electromagnetic fields generated by the magnetosphere and the ionosphere.
- Man-made noises generated by 60 Hz power lines and rail-ways.
- Ocean waves.
- Magnetic fields generated by sunspots.
- Noises generated by the vibrations of the sensor.
- Noises generated by the magnetic field measurement circuits.

Fig. 1 shows the typical frequency spectrum of the magnetic noise in the laboratory measured by a spectrum analyzer. We can see the strong 60 Hz noise by power lines and its harmonics, 1/f and white background noises.

Fowler[1] suggested that the change of measured magnetic fields at different locations can be modeled as a filter and concluded that the coherent magnetic field noises are dominant over the incoherent terms based on the experimental results.

In this paper, we developed digital signal processing algorithms of the GMF(Geological Magnetic Filter) to improve the signal to noise ratio of the magnetic detection system using the spatial coherency of the magnetic noises. In the proposed algorithm, two sensors, detector sensor and reference sensor located at a distance, measure the magnetic fields concurrently at the absence of the magnetic sources. After that, the correlations between the two fields are calculated in the frequency domain and the geological filter coefficients are calculated. The coefficients reflect the environments where the sensors are located. From the coefficients in the frequency domain, the FIR filter coefficients are calculated. Using the GMF, we can remove the coherent magnetic noises. The proposed algorithms can easily be implemented in real time.

This paper is described as follows.

In section II, we describe the theory of the GMF. In section III, computer simulation results are shown, which are followed by conclusions in section IV.

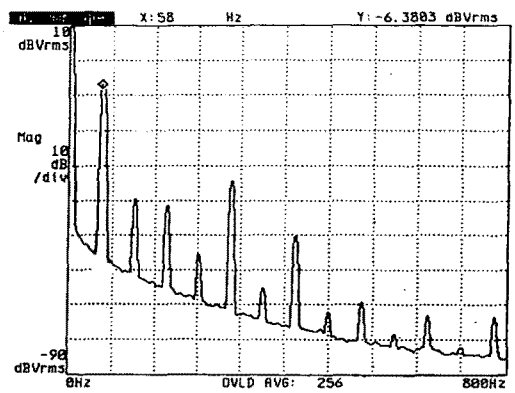

Fig. 1. Frequency spectrum of the measured magnetic field noise.

II. THEORY

Magnetic fields are generated by the magnetic moments which are originally due to the movements of the charged particles. The intensity of the magnetic fields drops rapidly as the distance from the source increases. For example, the field intensity by a magnetic dipole moment decreases in proportional to r^{-3}, where r is the distance from the source to the detect point. We can separate the measured magnetic fields into two components, long range field and the short

range field according to the distance from the magnetic source. If the distance between the detector and reference sensor is very short compared with the distance from the source, the difference of the measured magnetic fields between the two sensors is very small. But if the distance from the source is comparable to the sensor separations, the difference of the measured fields is very large.

The change of the measured long range magnetic fields between the detector and reference sensor is influenced by the environments where the sensors are located. The influence of the magnetic environments on the micropulsation fields can be modeled as follows[1].

We can model the magnetic environments where the reference sensor is located as a linear filter. The input of the filter is the micropulsation field with the orthogonal independent components, B^s_x and B^s_y. The characteristics of the filter is determined by the environments. The output of the filter is the reflected wave (B^r_x, B^r_y, B^r_z). And the measured micropulsation fields can be expressed as a sum of the input and reflected wave.

$$\begin{aligned} B_{R,x}(f) &= B^S_x(f) + B^r_x(f) \\ B_{R,y}(f) &= B^S_y(f) + B^r_y(f) \end{aligned} \tag{1}$$

The measured z direction field is the reflected wave.

$$B_{R,z}(f) = B^r_z(f) \tag{2}$$

From (1) and (2) the relation between the micropulsation input field and the measured magnetic field can be expressed as,

$$\begin{bmatrix} B_{R,x}(f) \\ B_{R,y}(f) \\ B_{R,z}(f) \end{bmatrix} = \begin{bmatrix} A_{11}(f) & A_{12}(f) \\ A_{21}(f) & A_{22}(f) \\ A_{31}(f) & A_{32}(f) \end{bmatrix} \begin{bmatrix} B^S_x(f) \\ B^S_y(f) \end{bmatrix} + \begin{bmatrix} B^S_x(f) \\ B^S_y(f) \\ 0 \end{bmatrix} \tag{3}$$

, where $A_{ij}(f)$ is the filter coefficient. (3) can be simplified as follows.

$$\begin{bmatrix} B_{R,x}(f) \\ B_{R,y}(f) \\ B_{R,z}(f) \end{bmatrix} = \begin{bmatrix} (1+A_{11}(f)) & A_{12}(f) \\ A_{21}(f) & (1+A_{22}(f)) \\ A_{31}(f) & A_{32}(f) \end{bmatrix} \begin{bmatrix} B^S_x(f) \\ B^S_y(f) \end{bmatrix} \tag{4}$$

The environments where the detector sensor is located are different from that around the reference sensor and expressed as another filter with different coefficients and the measured magnetic field at that point can be expressed as follows.

$$\begin{bmatrix} B_{D,x}(f) \\ B_{D,y}(f) \\ B_{D,z}(f) \end{bmatrix} = \begin{bmatrix} (1+B_{11}(f)) & B_{12}(f) \\ B_{21}(f) & (1+B_{22}(f)) \\ B_{31}(f) & B_{32}(f) \end{bmatrix} \begin{bmatrix} B^S_{D,x}(f) \\ B_{D,y}(f) \end{bmatrix} \tag{5}$$

The difference of input micropulsation fields at the two places can be expressed as,

$$\begin{aligned} B^S_{D,x}(f) &= B^S_x(f) + B_{N,x}(f) \\ B^S_{D,y}(f) &= B^S_y(f) + B_{N,y}(f) \end{aligned} \tag{6}$$

In (6), $B_{N,x}(f)$ and $B_{N,y}(f)$ are noise terms due to the spatial incoherency or gradient of the micropulsation field. Let's define the filter transformation operator C which reflects the difference of the environments around the two sensors.

$$\begin{bmatrix} C_{xx} & C_{xy} & C_{xz} \\ C_{yx} & C_{yy} & C_{yz} \\ C_{zx} & C_{zy} & C_{zz} \end{bmatrix} \begin{bmatrix} (1+A_{11}) & A_{12} \\ A_{21} & (1+A_{22}) \\ A_{31} & A_{32} \end{bmatrix} = \begin{bmatrix} (1+B_{11}) & B_{12} \\ B_{21} & (1+B_{22}) \\ B_{31} & B_{32} \end{bmatrix} \tag{7}$$

Then, we can obtain equation (8).

$$\begin{bmatrix} C_{xx} & C_{xy} & C_{xz} \\ C_{yx} & C_{yy} & C_{yz} \\ C_{zx} & C_{zy} & C_{zz} \end{bmatrix} \begin{bmatrix} B_{R,x}(f) \\ B_{R,y}(f) \\ B_{R,z}(f) \end{bmatrix} - \begin{bmatrix} B_{D,x}(f) \\ B_{D,y}(f) \\ B_{D,z}(f) \end{bmatrix} = -\begin{bmatrix} (1+B_{11}(f)) & B_{12}(f) \\ B_{21}(f) & (1+B_{22}(f)) \\ B_{31}(f) & B_{32}(f) \end{bmatrix} \begin{bmatrix} B_{N,x}(f) \\ B_{N,y}(f) \end{bmatrix} \tag{8}$$

In (8), the right terms are due to the incoherency of the source waves. Practically, it

can be generated due to the short range magnetic fields which strongly affect only one sensor. In realization of the geological magnetic filter, we obtain the filter coefficients C_{ij} which minimize the magnitude of right term in (8). When the filter coefficients C_{ij} are determined in the frequency domain, we can obtain the FIR filter coefficients in the time domain and the real time geological filter outputs can be calculated in the time domain.

III. COMPUTER SIMULATION RESULTS

To test the performance of the proposed GMF theory, we wrote a computer program using C language and simulated the GMF outputs under various conditions.

We can input the magnitude of the earth magnetic field, misalignments of two sensors, coherent and incoherent components of the noise, and the parameters for the construction of the geological filter such as the number of samples per data acquisition window, the number of data acquisition windows, and the number of FIR filter tabs. As we can see in Fig. 1, the background noises are composed of white noise and 1/f noise. The white and 1/f noise are shown in Fig. 2 in the frequency and time domain.

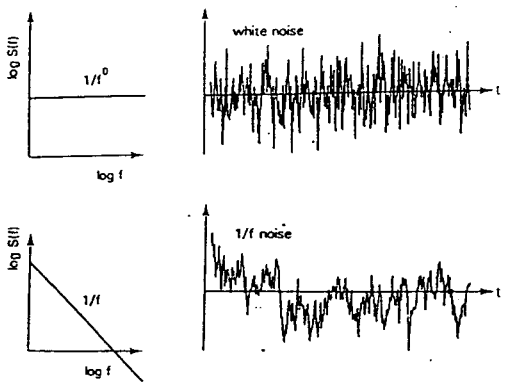

Fig. 2. White noise and 1/f noise in the frequency domain and time domain.

For the generation of the 1/f noise, we used the Fourier filtering method[2]. Input noise $\overline{x}(t_l)$ can be expressed in Fourier form.

$$\overline{x}(t_l) = \sum_{k=0}^{N-1} a_k e^{2\pi jkl/N} \tag{9}$$

If we sample $\overline{x}(t_l)$ in discrete time, there is a one to one correspondence between $\overline{x}(t_l)$ and a_k. If the spectral density S(f) of $\overline{x}(t)$ is proportional to $1/f^{\beta}$, following relation should be satisfied.

$$E(|a_k|^2) \propto \frac{1}{k^{\beta}} \tag{10}$$

In E(·) denotes the expected value. In Fourier filtering method, a_k is selected at random under the constraint of (10), which is followed by inverse Fourier transformations.

In Fig. 3, we show the numerical simulation results of time variation of the $B_{D,x}$, x component at the detector sensor, $B_{D,x}(t) - B_{R,x}(t)$ and the GMF output. Following values are assumed during simulations.

Average power of common mode noise : 1000 nT^2
Average power of differential mode noise : 50 nT^2
$B_{D,x}$ due to misalignment of x-axis of detector sensor : -104.4 nT
$B_{R,x}$ due to misalignment of x-axis of reference sensor : -52.2 nT
$B_{R,y}$ due to misalignment of y-axis of reference sensor : -0.17 nT
$B_{R,z}$ due to misalignment of z-axis of reference sensor : 90.73 nT

The calculated variance of GMF output is 142 nT^2, which has the S/N ratio improvements of 8.4dB compared to using a single sensor.

The calculated variance of $B_{D,x}(t) - B_{R,x}(t)$ is 50 nT^2, nearly three times less than that of GMF output. This is the expected result because we assumed no frequency dependence of the environments around the detector and reference

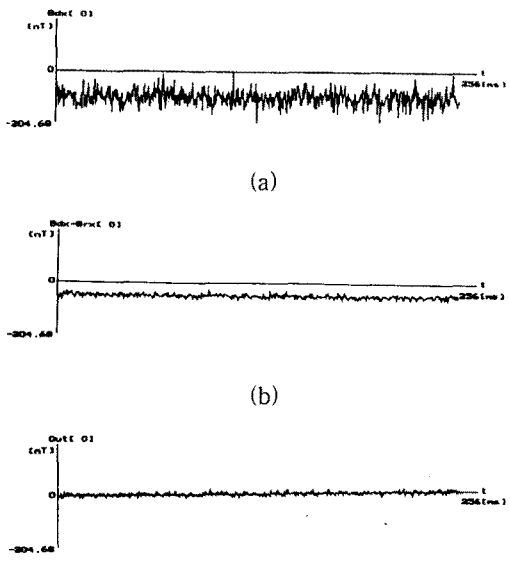

(a)

(b)

(c)

Fig. 3. Simulation results of the x component magnetic fields.
(a) $B_{D,x}(t)$ (b) $B_{D,x}(t)-B_{R,x}(t)$
(c) x component of GMF output

sensors. In RS-422 serial communications, where data are sent differentially, we can send data at a faster rate and to longer length than we can do using RS-232C lines[3]. This is because the difference voltage can be conserved when the common mode noises are applied to both differential signals. But, when the C_{ij} have frequency dependence, GMF can more effectively cancel out the coherent noises.

Also, we can see from Fig. 3 that the GMF compensate mean value of the misalignments of sensor orientation. The calculated mean value of GMF output is only -0.012 nT^2.

In Fig. 4 we show the GMF filter coefficients C_{xx} in frequency domain.

The object of GMF is to remove the coherent noise components measured at the detector sensor. Since we measure the magnetic fields at the detector and reference sensors at many windows and obtain the GMF coefficients using the least square method, it can be expected that GMF has the ability to cancel out the localized short range magnetic fields which affect strongly only one sensor. Fig. 5 shows the results for that case.

During the simulations for Fig. 5, localized magnetic field with Gaussian form in the frequency domain is applied to the detector sensor.

$$B_{D,x}(f) = \frac{B_{L0}}{\sqrt{2\pi\sigma}} \exp[-(f-\frac{f_s}{4})^2/2\sigma^2] + B_{D,x(coherent)} + B_{D,x(incoherent)},$$
$$f_s = 2Khz \tag{11}$$

In the time domain, the localized magnetic field component can be expressed as

$$B_{D,x(localized)}(t) = B_{L0} \exp[-\frac{2\pi^2\sigma^2 t^2}{2}] \exp[j\frac{\pi f_s t}{2}] \tag{12}$$

Fig. 5 shows the $C_{xx}(f)$. We can see the C_{xx} value is suppressed at the frequency around $f = f_s/4$.

For the results shown in Fig. 6, B_{L0} = 20 and $\sigma = \frac{f_s}{32}$ are assumed and the other parameters are the same as used in Fig. 3. Fig. 6(a) shows the $B_{D,x}(t)$, (b) shows the $B_{D,x}(t)-B_{R,x}(t)$, and (c) shows the GMF outputs for the x component. GMF output has mean value of -0.0553 nT and variance of 158 nT^2.

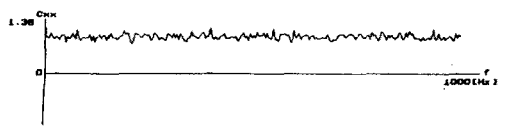

Fig. 4. Calculated $C_{xx}(f)$.

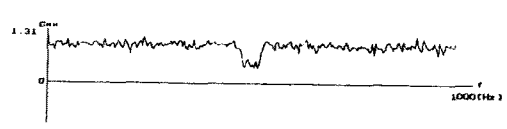

Fig. 5. Calculated $C_{xx}(f)$.

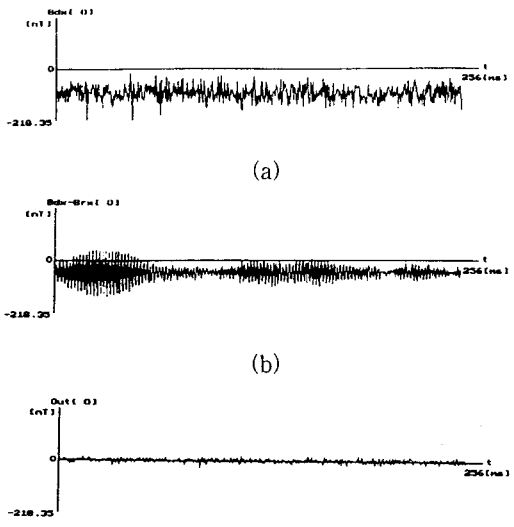

(a)

(b)

(c)

Fig. 6. Simulated magnetic fields variations when a localized field exist around only one sensor.
(a) $B_{D,x}(t)$ (b) $B_{D,x}(t)-B_{R,x}(t)$
(c) x component of GMF output

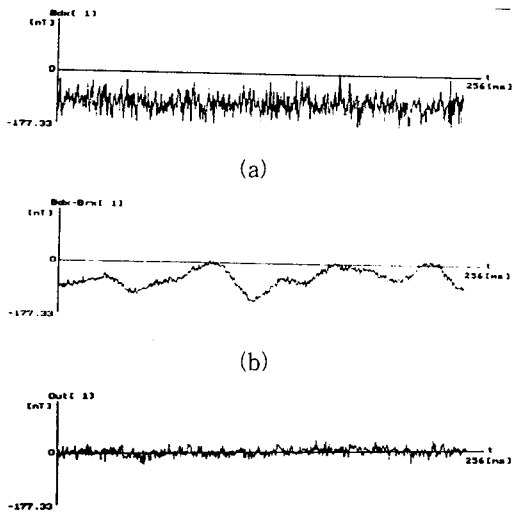

(a)

(b)

(c)

Fig. 7. Simulated magnetic fields variations when a localized field exists around only one sensor.
(a) $B_{D,x}(t)$ (b) $B_{D,x}(t)-B_{R,x}(t)$
(c) x component of GMF output

Fig. 7 shows the numerical simulation results when the following localized x components are applied to the detector sensor.

$$B_{D,x(localized)}(f) = \frac{B_{L0}}{\sqrt{2\pi\sigma}} \exp[-(f-\frac{f_s}{256})^2/2\sigma^2], \quad f_s = 2KHz \tag{13}$$

B_{L0} = 20, $\sigma = \frac{f_s}{32}$ are assumed and the other parameters are the same as used for Fig. 3. From the graph of $B_{D,x}(t)-B_{R,x}(t)$, we can see the large low frequency variations and these are canceled out at the GMF outputs. GMF results show that mean = -0.019 nT and variance = 177 nT^2.

For above simulation results, SNR improvement of GMF is shown in table 1.

Table 1. SNR improvement of GMF

Simulation No.	Variance (nT^2)		SNR improvement
	Detector sensor	Filter output	
1	975	142	8.4 dB
2	975	158	7.9 dB
3	975	177	7.4 dB

Also, we performed simulations when the magnetic source appears. Fig. 8 shows the orientations of two sensors and a moving magnetic source. It is assumed that the detector, reference sensors and the source are aligned along the x axis. The distance between detector and reference sensors is 10 m. At t=0, magnetic sensor is at x = 10m and moves at the constant speed of 10 m/s. Then, the magnetic field intensity B_{sig} measured at each sensor due to the magnetic moment of the source can be expressed as (14).

$$B_{sig} = \frac{C}{(x-x_0)^3} \tag{14}$$

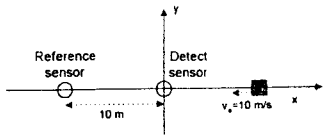

Fig. 8. Orientation of detector and reference sensors.

During the simulations, $C = 10^2 nT \cdot m^3$ and the magnetic environmental parameters as used for the results of Fig. 7 are used. Fig. 9 shows the results for $B_{D,x}(t)$, $B_{D,x}(t) - B_{R,x}(t)$, and GMF outputs.

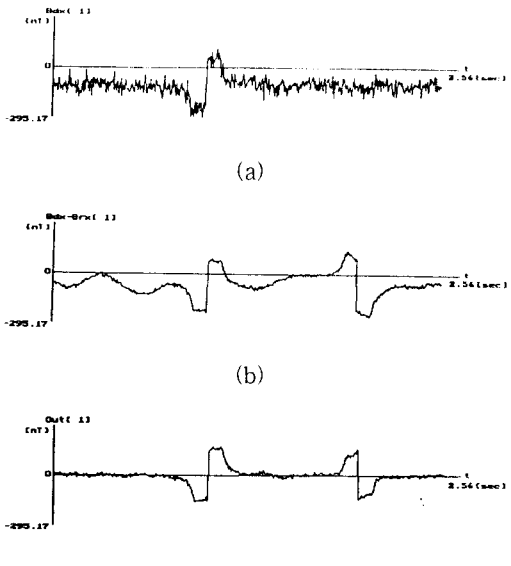

(a)

(b)

(c)

Fig. 9. Simulated results for magnetic fields.
(a) $B_{D,x}(t)$ (b) $B_{D,x}(t) - B_{R,x}(t)$
(c) x component of GMF output

IV. CONCLUSIONS

A theory of the GMF(Geological Magnetic Filter) that can improve the signal to noise ratio of the magnetic detection system has been presented and the numerical simulation results have been shown in this paper. GMF is constructed using two 3-axis magnetic sensors, detector sensor and reference sensors. The main object of GMF is to cancel out the coherent magnetic noises using two sensors. From the simulation results we could also observe that GMF can effectively remove the sensor misalignment effects and the localized noises due to short range magnetic sources. We constructed the GMF prototype and the measured results show excellent performances as anticipated in this work, which will be published soon.

REFERENCES

[1] B. Fowler, *A Study of the Geomagnetic Micropulsations Using Gradiomagnetic Techniques*, Ph. D dissertation, The University of Texas at Austin, 1973.

[2] Heinz-Otto Peitgen and Dietmar Saupe, *The Science of Fractal Images*, Springer-Verlag New York Inc., 1988.

[3] Horowitz and Hill, *The art of electronics*, Cambridge University Press, 1989.

著 者 紹 介

김 원 호

1963년 1월 22일생. 1985년 2월 경북대학교 전자공학과 졸업(공학사), 1988년 2월 경북대학교 대학원 전자공학과 졸업(공학석사), 1988년 6월 ~ 1993년 2월 한국전자통신연구원 연구원, 1993년 3월 ~ 현재 경북대학교 대학원 전자공학과 박사과정 수료, 1993년 3월 ~ 현재 동의공업전문대학 조교수. 주관심분야 : VLSI 설계, 디지털 신호처리

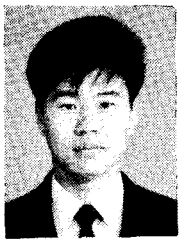

김 은 로

1968년 1월 16일생. 1990년 한국항공대학교 항공전자공학과 졸업(공학사), 1992년 동대학원 항공전자공학과 졸업(공학석사), 1992년 ~ 현재 국방과학연구소 연구원. 주관심분야 : 초전도 센서

양 창 섭

1966년 3월 31일생. 1988년 경북대학교 전자공학과 졸업(공학사), 1990년 동대학원 전자공학과 졸업(공학석사), 1990년 ~ 현재 국방과학연구소 연구원. 주관심분야 : 광섬유 센서

최 인 규

1972년 4월 28일생. 1995년 2월 경북대학교 전자공학과 졸업(공학사), 1997년 2월 경북대학교 대학원 전자공학과 졸업(공학석사), 1997년 ~ 현재 동대학원 박사과정. 주관심분야 : VLSI 설계, 디지털 신호처리

최 준 림

1964년 7월 1일생. 1986년 연세대학교 졸업(공학사), 1988년 Cornell University 졸업(공학석사), 1991년 University Of Minnesota졸업(공학박사), 1991년 ~ 1993년 금성중앙연구소, 1994년 ~ 1997년 LG 전자연구소 선임 연구원, 1997년 ~ 현재 경북대학교 전자·전기공학부 전임강사.

박 종 식

『센서학회지 제5권 제3호』 논문 96-5-3-07 p. 54 참조. 현재 경북대학교 전자·전기공학부 교수